Can inflation be falsified?

L. Sriramkumar

Department of Physics, Indian Institute of Technology Madras, Chennai

Colloquium

National Centre for Radio Astrophysics, Pune

April 10, 2017

Plan of the talk

1. The inflationary paradigm
2. The scalar and tensor power spectra generated during inflation
3. Constraints from Planck
4. The Maldacena formalism to evaluate the inflationary scalar bispectrum
5. Constraints on non-Gaussianities
6. BINGO: An efficient code to numerically compute the bispectrum
7. Are bouncing models viable?
8. Summary and outlook

Plan of the talk

The resolution of the horizon problem in inflation

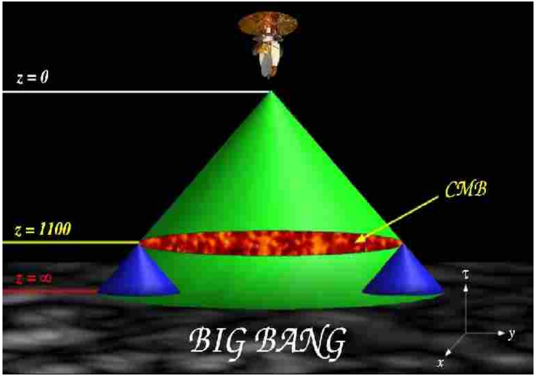

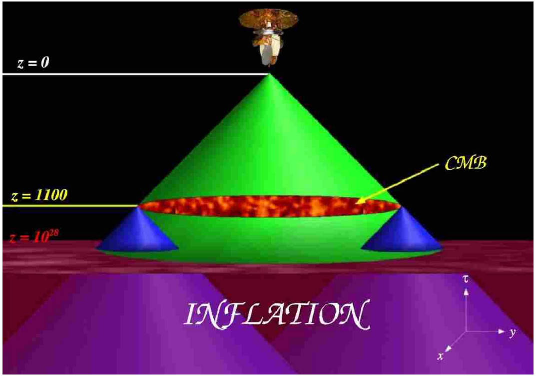

Left: The radiation from the CMB arriving at us from regions separated by more than the Hubble radius at the last scattering surface (which subtends an angle of about 1° today) could not have interacted before decoupling.

[1] Images from W. Kinney, astro-ph/0301448.

The resolution of the horizon problem in inflation

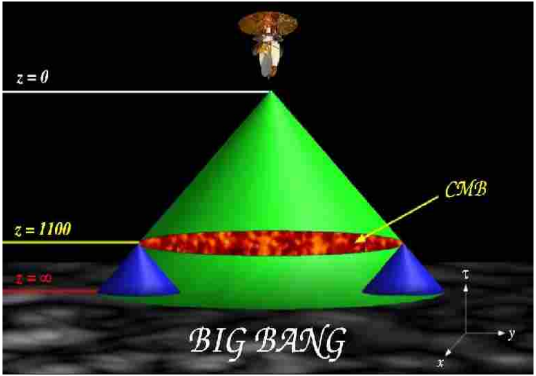

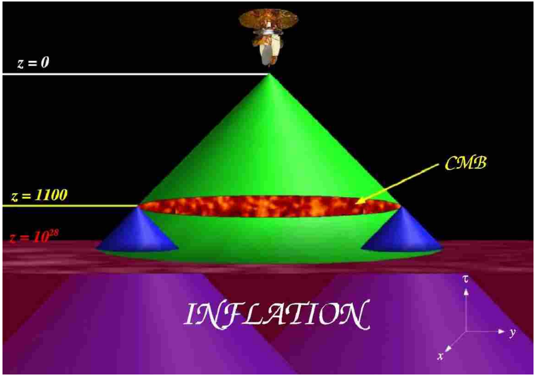

Left: The radiation from the CMB arriving at us from regions separated by more than the Hubble radius at the last scattering surface (which subtends an angle of about 1° today) could not have interacted before decoupling.

Right: An illustration of how an early and sufficiently long epoch of inflation helps in resolving the horizon problem[1].

[1] Images from W. Kinney, astro-ph/0301448.

Bringing the modes inside the Hubble radius

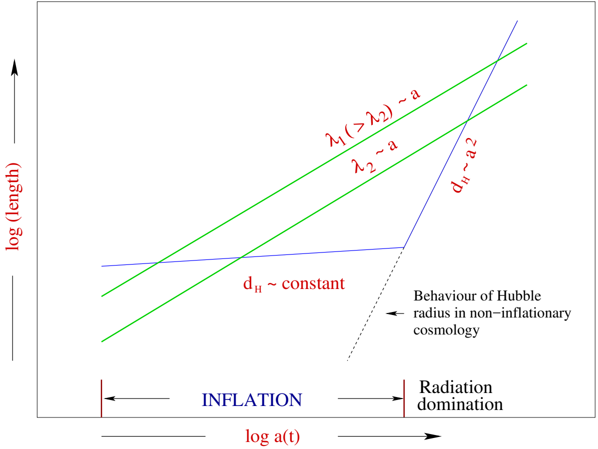

The behavior of the physical wavelength $\lambda_{\rm P} \propto a$ (the green lines) and the Hubble radius H^{-1} (the blue line) during inflation and the radiation dominated epochs[2].

Back to bounce

[2] See, for example, E. W. Kolb and M. S. Turner, *The Early Universe* (Addison-Wesley Publishing Company, New York, 1990), Fig. 8.4.

Driving inflation with scalar fields

If we require that $\lambda_{\rm P} < d_{\rm H}$ at a sufficiently early time, then we need to have an epoch wherein $\lambda_{\rm P}$ decreases faster than the Hubble scale *as we go back in time*, i.e. a regime during which

$$-\frac{\mathrm{d}}{\mathrm{d}\,t}\left(\frac{\lambda_{\rm P}}{d_{\rm H}}\right) < 0 \quad \Rightarrow \quad \ddot{a} > 0.$$

[3] See, for instance, B. A. Bassett, S. Tsujikawa and D. Wands, Rev. Mod. Phys. **78**, 537 (2006).

Driving inflation with scalar fields

If we require that $\lambda_{\rm P} < d_{\rm H}$ at a sufficiently early time, then we need to have an epoch wherein $\lambda_{\rm P}$ decreases faster than the Hubble scale *as we go back in time*, i.e. a regime during which

$$-\frac{\mathrm{d}}{\mathrm{d}\,t}\left(\frac{\lambda_{\rm P}}{d_{\rm H}}\right) < 0 \quad \Rightarrow \quad \ddot{a} > 0.$$

From the Friedmann equations, we then require that, during this epoch,

$$(\rho + 3\,p) < 0.$$

Back to the bounce

[3]See, for instance, B. A. Bassett, S. Tsujikawa and D. Wands, Rev. Mod. Phys. **78**, 537 (2006).

Driving inflation with scalar fields

If we require that $\lambda_{\rm P} < d_{\rm H}$ at a sufficiently early time, then we need to have an epoch wherein $\lambda_{\rm P}$ decreases faster than the Hubble scale *as we go back in time*, i.e. a regime during which

$$-\frac{{\rm d}}{{\rm d}\,t}\left(\frac{\lambda_{\rm P}}{d_{\rm H}}\right) < 0 \quad \Rightarrow \quad \ddot{a} > 0.$$

From the Friedmann equations, we then require that, during this epoch,

$$(\rho + 3\,p) < 0.$$

Back to the bounce

In the case of canonical scalar fields, this condition simplifies to

$$\dot{\phi}^2 < V(\phi).$$

[3]See, for instance, B. A. Bassett, S. Tsujikawa and D. Wands, Rev. Mod. Phys. **78**, 537 (2006).

Driving inflation with scalar fields

If we require that $\lambda_{\rm P} < d_{\rm H}$ at a sufficiently early time, then we need to have an epoch wherein $\lambda_{\rm P}$ decreases faster than the Hubble scale *as we go back in time*, i.e. a regime during which

$$-\frac{{\rm d}}{{\rm d}\,t}\left(\frac{\lambda_{\rm P}}{d_{\rm H}}\right) < 0 \quad \Rightarrow \quad \ddot{a} > 0.$$

From the Friedmann equations, we then require that, during this epoch,

$$(\rho + 3\,p) < 0.$$

Back to the bounce

In the case of canonical scalar fields, this condition simplifies to

$$\dot{\phi}^2 < V(\phi).$$

This condition can be achieved if the scalar field ϕ is initially displaced from a minima of the potential, and inflation will end when the field approaches a minima with zero or negligible potential energy[3].

[3] See, for instance, B. A. Bassett, S. Tsujikawa and D. Wands, Rev. Mod. Phys. **78**, 537 (2006).

A variety of potentials to choose from

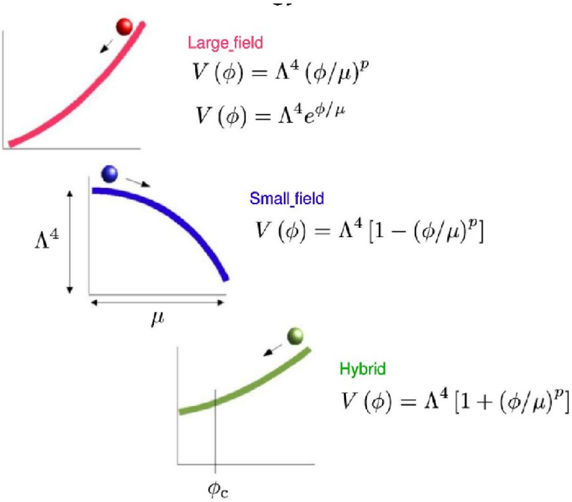

A variety of scalar field potentials have been considered to drive inflation[4]. Often, these potentials are classified as small field, large field and hybrid models.

[4] Image from W. Kinney, astro-ph/0301448.

Proliferation of inflationary models

5-dimensional assisted inflation
anisotropic brane inflation
anomaly-induced inflation
assisted inflation
assisted chaotic inflation
boundary inflation
brane inflation
brane-assisted inflation
brane gas inflation
brane-antibrane inflation
braneworld inflation
Brans-Dicke chaotic inflation
Brans-Dicke inflation
bulky brane inflation
chaotic hybrid inflation
chaotic inflation
chaotic new inflation
D-brane inflation
D-term inflation
dilaton-driven inflation
dilaton-driven brane inflation
double inflation
double D-term inflation
dual inflation
dynamical inflation
dynamical SUSY inflation
eternal inflation
extended inflation
extended open inflation
extended warm inflation
extra dimensional inflation
F-term inflation
F-term hybrid inflation
false vacuum inflation
false vacuum chaotic inflation
fast-roll inflation
first order inflation
gauged inflation
generalised inflation
generalized assisted inflation
generalized slow-roll inflation
gravity driven inflation
Hagedorn inflation
higher-curvature inflation
hybrid inflation
hyperextended inflation
induced gravity inflation
induced gravity open inflation
intermediate inflation
inverted hybrid inflation
isocurvature inflation
K inflation
kinetic inflation
lambda inflation
large field inflation
late D-term inflation
late-time mild inflation
low-scale inflation
low-scale supergravity inflation
M-theory inflation
mass inflation
massive chaotic inflation
moduli inflation
multi-scalar inflation
multiple inflation
multiple-field slow-roll inflation
multiple-stage inflation
natural inflation
natural Chaotic inflation
natural double inflation
natural supergravity inflation
new inflation
next-to-minimal supersymmetric hybrid inflation
non-commutative inflation
non-slow-roll inflation
nonminimal chaotic inflation
old inflation
open hybrid inflation
open inflation
oscillating inflation
polynomial chaotic inflation
polynomial hybrid inflation
power-law inflation
pre-Big-Bang inflation
primary inflation
primordial inflation
quasi-open inflation
quintessential inflation
R-invariant topological inflation
rapid asymmetric inflation
running inflation
scalar-tensor gravity inflation
scalar-tensor stochastic inflation
Seiberg-Witten inflation
single-bubble open inflation
spinodal inflation
stable starobinsky-type inflation
steady-state eternal inflation
steep inflation
stochastic inflation
string-forming open inflation
successful D-term inflation
supergravity inflation
supernatural inflation
superstring inflation
supersymmetric hybrid inflation
supersymmetric inflation
supersymmetric topological inflation
supersymmetric new inflation
synergistic warm inflation
TeV-scale hybrid inflation

A (partial?) list of ever-increasing number of inflationary models[5]. Actually, it may not even be possible to rule out some of these models!

[5] From E. P. S. Shellard, *The future of cosmology: Observational and computational prospects*, in *The Future of Theoretical Physics and Cosmology*, Eds. G. W. Gibbons, E. P. S. Shellard and S. J. Rankin (Cambridge University Press, Cambridge, England, 2003).

Plan of the talk

The character of the perturbations

In a Friedmann universe, the perturbations in the metric and the matter can be classified according to their behavior with respect to local rotation of the spatial coordinates on hypersurfaces of constant time as follows[6]:

- Scalar perturbations – Density and pressure perturbations
- Vector perturbations – Rotational velocity fields
- Tensor perturbations – Gravitational waves

[6] See, for instance, L. Sriramkumar, Curr. Sci. **97**, 868 (2009).

The character of the perturbations

In a Friedmann universe, the perturbations in the metric and the matter can be classified according to their behavior with respect to local rotation of the spatial coordinates on hypersurfaces of constant time as follows[6]:

- Scalar perturbations – Density and pressure perturbations
- Vector perturbations – Rotational velocity fields
- Tensor perturbations – Gravitational waves

The metric perturbations are related to the matter perturbations through the first order Einstein's equations.

[6] See, for instance, L. Sriramkumar, Curr. Sci. **97**, 868 (2009).

The character of the perturbations

In a Friedmann universe, the perturbations in the metric and the matter can be classified according to their behavior with respect to local rotation of the spatial coordinates on hypersurfaces of constant time as follows[6]:

- ✦ Scalar perturbations – Density and pressure perturbations
- ✦ Vector perturbations – Rotational velocity fields
- ✦ Tensor perturbations – Gravitational waves

The metric perturbations are related to the matter perturbations through the first order Einstein's equations.

Inflation does not produce any vector perturbations, while the tensor perturbations can be generated even in the absence of sources.

[6] See, for instance, L. Sriramkumar, Curr. Sci. **97**, 868 (2009).

The character of the perturbations

In a Friedmann universe, the perturbations in the metric and the matter can be classified according to their behavior with respect to local rotation of the spatial coordinates on hypersurfaces of constant time as follows[6]:

- Scalar perturbations – Density and pressure perturbations
- Vector perturbations – Rotational velocity fields
- Tensor perturbations – Gravitational waves

The metric perturbations are related to the matter perturbations through the first order Einstein's equations.

Inflation does not produce any vector perturbations, while the tensor perturbations can be generated even in the absence of sources.

It is the fluctuations in the inflaton field ϕ that act as the seeds for the scalar perturbations that are primarily responsible for the anisotropies in the CMB and, eventually, the present day inhomogeneities.

[6] See, for instance, L. Sriramkumar, Curr. Sci. **97**, 868 (2009).

The quadratic action governing the perturbations

One can show that, at the quadratic order, the action governing the curvature perturbation $\mathcal{R}$ and the tensor perturbation γ_{ij} are given by[7]

$$\mathcal{S}_2[\mathcal{R}] = \frac{1}{2}\int \mathrm{d}\eta \int \mathrm{d}^3\boldsymbol{x}\; z^2\,\left[\mathcal{R}'^2 - (\partial\mathcal{R})^2\right],$$

$$\mathcal{S}_2[\gamma_{ij}] = \frac{M_{\mathrm{Pl}}^2}{8}\int \mathrm{d}\eta \int \mathrm{d}^3\boldsymbol{x}\; a^2\,\left[\gamma_{ij}'^{\,2} - (\partial\gamma_{ij})^2\right].$$

Back to the cubic action

[7] V. F. Mukhanov, H. A. Feldman and R. H. Brandenberger, Phys. Rep. **215**, 203 (1992).

The quadratic action governing the perturbations

One can show that, at the quadratic order, the action governing the curvature perturbation $\mathcal{R}$ and the tensor perturbation γ_{ij} are given by[7]

$$\mathcal{S}_2[\mathcal{R}] = \frac{1}{2}\int \mathrm{d}\eta \int \mathrm{d}^3\boldsymbol{x}\; z^2\, \left[\mathcal{R}'^2 - (\partial\mathcal{R})^2\right],$$

$$\mathcal{S}_2[\gamma_{ij}] = \frac{M_{_{\mathrm{Pl}}}^2}{8}\int \mathrm{d}\eta \int \mathrm{d}^3\boldsymbol{x}\; a^2\, \left[\gamma_{ij}'^{\,2} - (\partial\gamma_{ij})^2\right].$$

Back to the cubic action

These actions lead to the following equations of motion governing the scalar and tensor modes, say, f_k and h_k:

$$f_k'' + 2\,\frac{z'}{z}\, f_k' + k^2\, f_k = 0,$$

$$h_k'' + 2\,\frac{a'}{a}\, h_k' + k^2\, h_k = 0,$$

where $z = a\, M_{_{\mathrm{Pl}}}\, \sqrt{2\,\epsilon_1}$, with $\epsilon_1 = -\,\mathrm{d}\ln H/\mathrm{d}N$ being the first slow roll parameter.

[7] V. F. Mukhanov, H. A. Feldman and R. H. Brandenberger, Phys. Rep. **215**, 203 (1992).

Quantization of the scalar and tensor perturbations

On quantization, the operators $\hat{\mathcal{R}}(\eta, \boldsymbol{x})$ and $\hat{\gamma}_{ij}(\eta, \boldsymbol{x})$ representing the scalar and the tensor perturbations can be expressed in terms of the corresponding Fourier modes f_k and g_k as[8]

$$\begin{aligned}\hat{\mathcal{R}}(\eta, \boldsymbol{x}) &= \int \frac{\mathrm{d}^3\boldsymbol{k}}{(2\,\pi)^{3/2}}\, \hat{\mathcal{R}}_{\boldsymbol{k}}(\eta)\, \mathrm{e}^{i\,\boldsymbol{k}\cdot\boldsymbol{x}} = \int \frac{\mathrm{d}^3\boldsymbol{k}}{(2\,\pi)^{3/2}}\, \left[\hat{a}_{\boldsymbol{k}}\, f_k(\eta)\, \mathrm{e}^{i\,\boldsymbol{k}\cdot\boldsymbol{x}} + \hat{a}^{\dagger}_{\boldsymbol{k}}\, f^{*}_k(\eta)\, \mathrm{e}^{-i\,\boldsymbol{k}\cdot\boldsymbol{x}}\right],\\ \hat{\gamma}_{ij}(\eta, \boldsymbol{x}) &= \int \frac{\mathrm{d}^3\boldsymbol{k}}{(2\,\pi)^{3/2}}\, \hat{\gamma}^{\boldsymbol{k}}_{ij}(\eta)\, \mathrm{e}^{i\,\boldsymbol{k}\cdot\boldsymbol{x}}\\ &= \sum_s \int \frac{\mathrm{d}^3\boldsymbol{k}}{(2\,\pi)^{3/2}}\, \left[\hat{b}^{s}_{\boldsymbol{k}}\, \varepsilon^{s}_{ij}(\boldsymbol{k})\, g_k(\eta)\, \mathrm{e}^{i\,\boldsymbol{k}\cdot\boldsymbol{x}} + \hat{b}^{s\dagger}_{\boldsymbol{k}}\, \varepsilon^{s*}_{ij}(\boldsymbol{k})\, g^{*}_k(\eta)\, \mathrm{e}^{-i\,\boldsymbol{k}\cdot\boldsymbol{x}}\right].\end{aligned}$$

[8] See, for instance, L. Sriramkumar, Curr. Sci. **97**, 868 (2009).

Quantization of the scalar and tensor perturbations

On quantization, the operators $\hat{\mathcal{R}}(\eta, \boldsymbol{x})$ and $\hat{\gamma}_{ij}(\eta, \boldsymbol{x})$ representing the scalar and the tensor perturbations can be expressed in terms of the corresponding Fourier modes f_k and g_k as[8]

$$\hat{\mathcal{R}}(\eta, \boldsymbol{x}) = \int \frac{\mathrm{d}^3\boldsymbol{k}}{(2\,\pi)^{3/2}}\, \hat{\mathcal{R}}_{\boldsymbol{k}}(\eta)\, \mathrm{e}^{i\,\boldsymbol{k}\cdot\boldsymbol{x}} = \int \frac{\mathrm{d}^3\boldsymbol{k}}{(2\,\pi)^{3/2}} \left[\hat{a}_{\boldsymbol{k}}\, f_k(\eta)\, \mathrm{e}^{i\,\boldsymbol{k}\cdot\boldsymbol{x}} + \hat{a}_{\boldsymbol{k}}^{\dagger}\, f_k^{*}(\eta)\, \mathrm{e}^{-i\,\boldsymbol{k}\cdot\boldsymbol{x}}\right],$$

$$\hat{\gamma}_{ij}(\eta, \boldsymbol{x}) = \int \frac{\mathrm{d}^3\boldsymbol{k}}{(2\,\pi)^{3/2}}\, \hat{\gamma}_{ij}^{\boldsymbol{k}}(\eta)\, \mathrm{e}^{i\,\boldsymbol{k}\cdot\boldsymbol{x}}$$

$$= \sum_s \int \frac{\mathrm{d}^3\boldsymbol{k}}{(2\,\pi)^{3/2}} \left[\hat{b}_{\boldsymbol{k}}^{s}\, \varepsilon_{ij}^{s}(\boldsymbol{k})\, g_k(\eta)\, \mathrm{e}^{i\,\boldsymbol{k}\cdot\boldsymbol{x}} + \hat{b}_{\boldsymbol{k}}^{s\dagger}\, \varepsilon_{ij}^{s*}(\boldsymbol{k})\, g_k^{*}(\eta)\, \mathrm{e}^{-i\,\boldsymbol{k}\cdot\boldsymbol{x}}\right].$$

In these decompositions, the operators $(\hat{a}_{\boldsymbol{k}}, \hat{a}_{\boldsymbol{k}}^{\dagger})$ and $(\hat{b}_{\boldsymbol{k}}^{s}, \hat{b}_{\boldsymbol{k}}^{s\dagger})$ satisfy the standard commutation relations, while the quantity $\varepsilon_{ij}^{s}(\boldsymbol{k})$ represents the transverse and traceless polarization tensor describing the gravitational waves.

[8] See, for instance, L. Sriramkumar, Curr. Sci. **97**, 868 (2009).

The scalar and tensor power spectra

The dimensionless scalar and tensor power spectra $\mathcal{P}_{_{\rm S}}(k)$ and $\mathcal{P}_{_{\rm T}}(k)$ are defined in terms of the correlation functions of the Fourier modes $\hat{\mathcal{R}}_{\boldsymbol{k}}$ and $\hat{\gamma}_{mn}^{\boldsymbol{k}}$ as follows:

$$\langle \hat{\mathcal{R}}_{\boldsymbol{k}}(\eta)\, \hat{\mathcal{R}}_{\boldsymbol{k}'}(\eta)\rangle = \frac{(2\,\pi)^2}{2\,k^3}\, \mathcal{P}_{_{\rm S}}(k)\; \delta^{(3)}\left(\boldsymbol{k}+\boldsymbol{k}'\right),$$

$$\langle \hat{\gamma}_{m_1n_1}^{\boldsymbol{k}}(\eta)\, \hat{\gamma}_{m_2n_2}^{\boldsymbol{k}'}(\eta)\rangle = \frac{(2\,\pi)^2}{8\,k^3}\, \Pi_{m_1n_1,m_2n_2}^{\boldsymbol{k}}\; \mathcal{P}_{_{\rm T}}(k)\; \delta^{3}\left(\boldsymbol{k}+\boldsymbol{k}'\right),$$

where $\Pi_{m_1n_1,m_2n_2}^{\boldsymbol{k}} = \sum_s\, \varepsilon_{m_1n_1}^{s}(\boldsymbol{k})\, \varepsilon_{m_2n_2}^{s*}(\boldsymbol{k})$.

The scalar and tensor power spectra

The dimensionless scalar and tensor power spectra $\mathcal{P}_{_{\rm S}}(k)$ and $\mathcal{P}_{_{\rm T}}(k)$ are defined in terms of the correlation functions of the Fourier modes $\hat{\mathcal{R}}_{\boldsymbol{k}}$ and $\hat{\gamma}_{mn}^{\boldsymbol{k}}$ as follows:

$$\langle \hat{\mathcal{R}}_{\boldsymbol{k}}(\eta)\, \hat{\mathcal{R}}_{\boldsymbol{k}'}(\eta)\rangle = \frac{(2\,\pi)^2}{2\,k^3}\, \mathcal{P}_{_{\rm S}}(k)\; \delta^{(3)}\left(\boldsymbol{k}+\boldsymbol{k}'\right),$$

$$\langle \hat{\gamma}_{m_1 n_1}^{\boldsymbol{k}}(\eta)\, \hat{\gamma}_{m_2 n_2}^{\boldsymbol{k}'}(\eta)\rangle = \frac{(2\,\pi)^2}{8\,k^3}\, \Pi_{m_1 n_1, m_2 n_2}^{\boldsymbol{k}}\; \mathcal{P}_{_{\rm T}}(k)\; \delta^{3}\left(\boldsymbol{k}+\boldsymbol{k}'\right),$$

where $\Pi_{m_1 n_1, m_2 n_2}^{\boldsymbol{k}} = \sum_s\, \varepsilon_{m_1 n_1}^{s}(\boldsymbol{k})\, \varepsilon_{m_2 n_2}^{s*}(\boldsymbol{k})$.

In the Bunch-Davies vacuum, say, $|0\rangle$, which is defined as $\hat{a}_{\boldsymbol{k}}|0\rangle = 0$ and $\hat{b}_{\boldsymbol{k}}^{s}|0\rangle = 0\; \forall\; \boldsymbol{k}$ and s, we can express the power spectra in terms of the quantities f_k and g_k as

$$\mathcal{P}_{_{\rm S}}(k) = \frac{k^3}{2\,\pi^2}\, |f_k|^2, \quad \mathcal{P}_{_{\rm T}}(k) = 4\, \frac{k^3}{2\,\pi^2}\, |h_k|^2.$$

With the initial conditions imposed in the sub-Hubble domain, *viz.* when $k/(a\,H) \gg 1$, these spectra are to be evaluated on super-Hubble scales, *i.e.* as $k/(a\,H) \ll 1$.

From inside the Hubble radius to super-Hubble scales

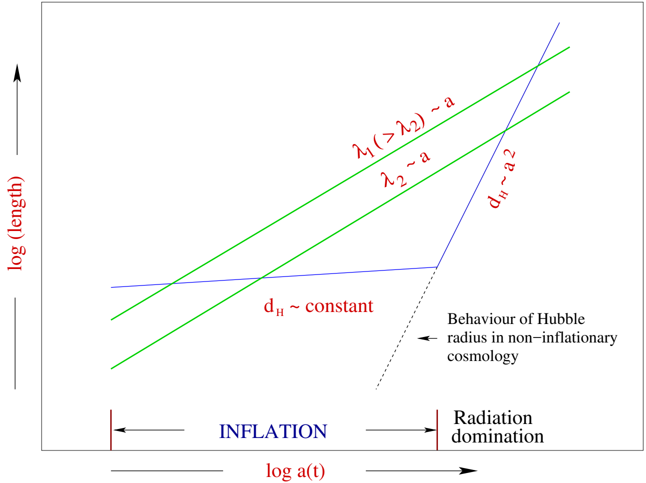

The initial conditions are imposed in the sub-Hubble regime when the modes are well inside the Hubble radius (*viz.* when $k/(a\,H) \gg 1$) and the power spectra are evaluated when they sufficiently outside (*i.e.* as $k/(a\,H) \ll 1$).

Typical evolution of the scalar modes

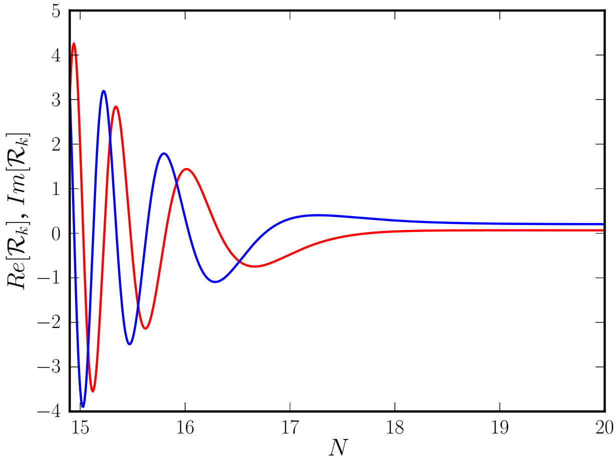

Typical evolution of the real and the imaginary parts of the scalar modes during slow roll inflation. The mode considered leaves the Hubble radius at about 18 e-folds[9].

[9] Figure from V. Sreenath, *Computation and characteristics of inflationary three-point functions*, Ph.D. Thesis, Indian Institute of Technology Madras, Chennai, India (2015).

Spectral indices and the tensor-to-scalar ratio

While comparing with the observations, for convenience, one often uses the following power law, template scalar and the tensor spectra:

$$\mathcal{P}_{\mathrm{S}}(k) = \mathcal{A}_{\mathrm{S}} \left(\frac{k}{k_*}\right)^{n_{\mathrm{S}}-1}, \qquad \mathcal{P}_{\mathrm{T}}(k) = \mathcal{A}_{\mathrm{T}} \left(\frac{k}{k_*}\right)^{n_{\mathrm{T}}},$$

with the spectral indices n_{S} and n_{T} assumed to be constant.

Spectral indices and the tensor-to-scalar ratio

While comparing with the observations, for convenience, one often uses the following power law, template scalar and the tensor spectra:

$$\mathcal{P}_{_{\rm S}}(k) = \mathcal{A}_{_{\rm S}}\, \left(\frac{k}{k_\ast}\right)^{n_{\rm S}-1}, \qquad \mathcal{P}_{_{\rm T}}(k) = \mathcal{A}_{_{\rm T}}\, \left(\frac{k}{k_\ast}\right)^{n_{\rm T}},$$

with the spectral indices $n_{_{\rm S}}$ and $n_{_{\rm T}}$ assumed to be constant.

The tensor-to-scalar ratio r is defined as

$$r(k) = \frac{\mathcal{P}_{_{\rm T}}(k)}{\mathcal{P}_{_{\rm S}}(k)}$$

and it is usual to further set $r = -8\, n_{_{\rm T}}$, *viz.* the so-called consistency relation, which is valid during slow roll inflation.

Theoretical angular power spectra[10]

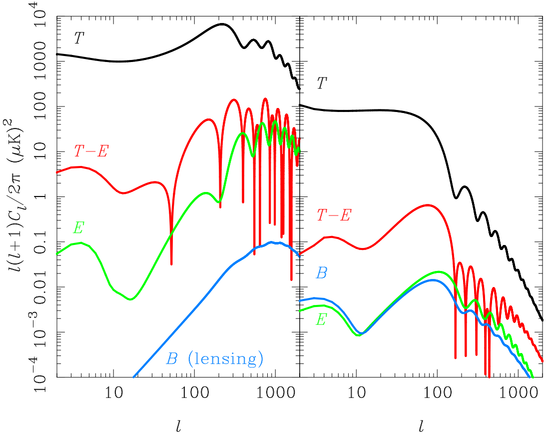

The *theoretically* computed, CMB angular power and cross-correlation spectra – temperature (T, in black), E (in green), B (in blue), and T-E (in red) – arising due to scalars (on the left) and tensors (on the right) corresponding to a tensor-to-scalar ratio of $r = 0.24$. The B-mode spectrum induced by weak gravitational lensing has also been shown (in blue) in the panel on the left.

[10] Figure from A. Challinor, arXiv:1210.6008 [astro-ph.CO].

CMB anisotropies as seen by Planck

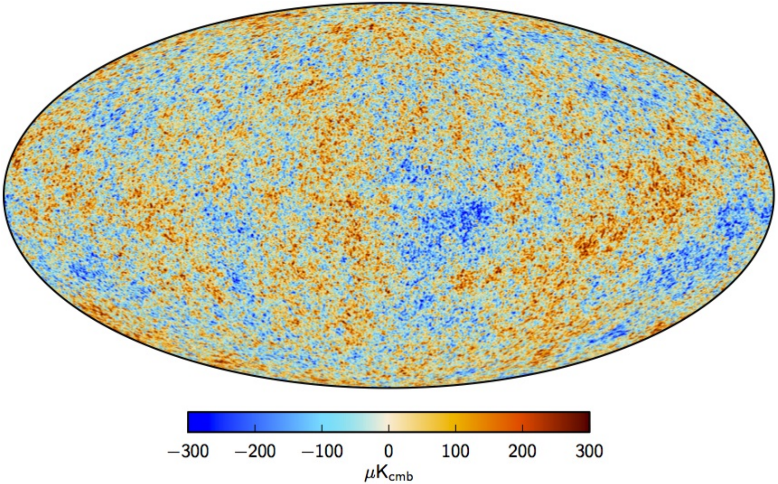

CMB intensity map at $5'$ resolution derived from the joint analysis of Planck, WMAP, and $408\,\mathrm{MHz}$ observations[11].

[11] Planck Collaboration (R. Adam *et al.*), Astron. Astrophys. **594**, A1 (2016).

CMB TT angular power spectrum from Planck

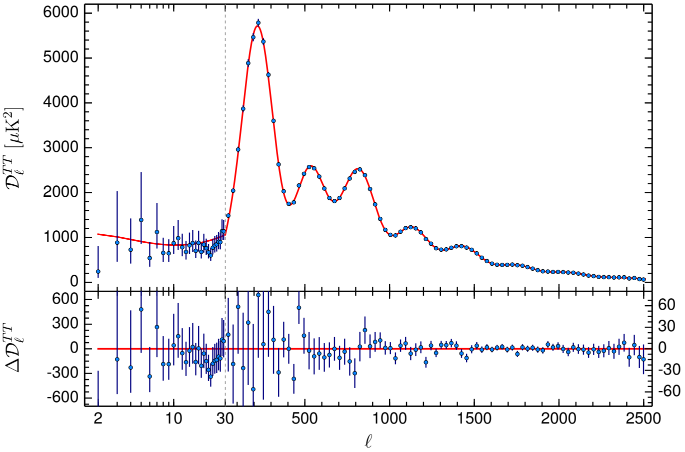

The CMB TT angular power spectrum from the Planck 2015 data (the blue dots with error bars) and the theoretical, best fit ΛCDM model with a power law primordial spectrum (the solid red curve)[12].

[12] Planck Collaboration (P. A. R. Ade *et al.*), Astron. Astrophys. **594**, A20 (2016).

CMB TE and EE angular power spectra from Planck

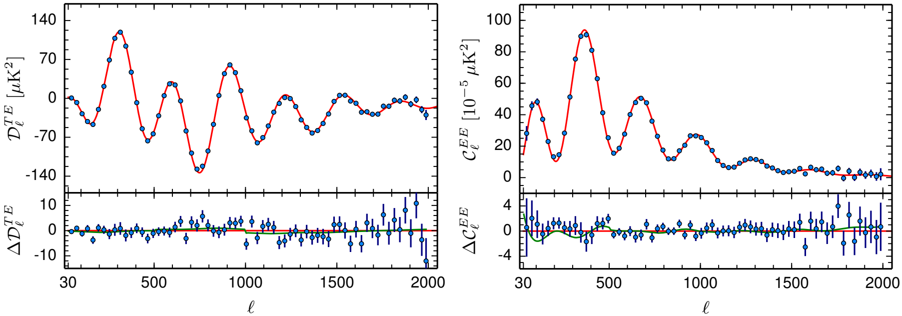

The CMB TE (on the left) and EE (on the right) angular power spectra from the Planck 2015 data (the blue dots with error bars) and the theoretical, best fit ΛCDM model with a power law primordial spectrum (the solid red curves)[13].

[13] Planck Collaboration (P. A. R. Ade *et al.*), Astron. Astrophys. **594**, A20 (2016).

[14] D. N. Spergel and M. Zaldarriaga, Phys. Rev. Lett. **79**, 2180 (1997).

CMB TE and EE angular power spectra from Planck

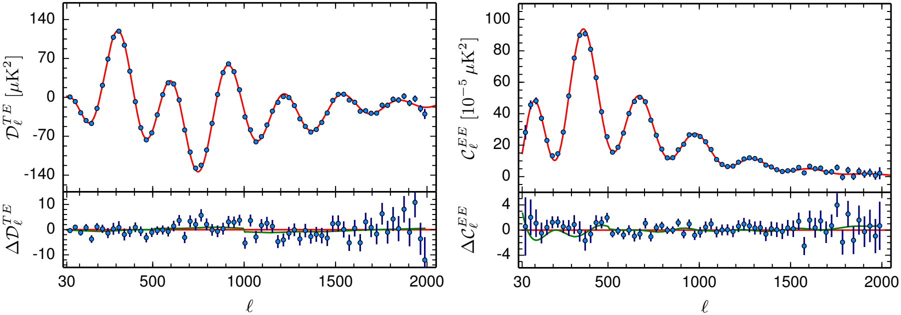

The CMB TE (on the left) and EE (on the right) angular power spectra from the Planck 2015 data (the blue dots with error bars) and the theoretical, best fit ΛCDM model with a power law primordial spectrum (the solid red curves)[13].

The large angle ($50 < \ell < 150$) TE anti-correlation detected by Planck (and earlier by WMAP) is a distinctive signature of primordial, super-Hubble, adiabatic perturbations[14].

[13] Planck Collaboration (P. A. R. Ade *et al.*), Astron. Astrophys. **594**, A20 (2016).

[14] D. N. Spergel and M. Zaldarriaga, Phys. Rev. Lett. **79**, 2180 (1997).

Joint constraints on r and $n_{\rm s}$

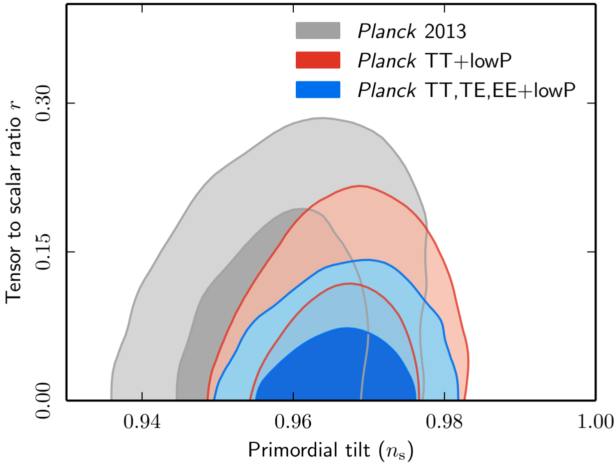

Marginalized joint confidence contours for $(n_{\rm s}, r)$, at the $68\,\%$ and $95\,\%$ CL, in the presence of running of the spectral indices, and for the same combinations of data as in the previous figure[15].

[15] Planck Collaboration (P. A. R. Ade *et al.*), Astron. Astrophys. **594**, A20 (2016).

Specific inflationary models of interest I

Power law potentials: In power law potentials of the following form[16]:

$$V(\phi) = \lambda\, M_{_{\mathrm{Pl}}}^4\, \left(\phi/M_{_{\mathrm{Pl}}}\right)^n,$$

inflation occurs for large values of the field, *i.e.* $\phi > M_{_{\mathrm{Pl}}}$.

[16] A. D. Linde, Phys. Lett. B **129**, 177 (1983).

[17] L. Boubekeur and D. Lyth, JCAP **0507**, 010 (2005).

[18] K. Freese, J. .A. Frieman and A. V. Olinto, Phys. Rev. Lett. **65**, 3233 (1990).

Specific inflationary models of interest I

Power law potentials: In power law potentials of the following form[16]:

$$V(\phi) = \lambda\, M_{_{\rm Pl}}^4\, \left(\phi/M_{_{\rm Pl}}\right)^n,$$

inflation occurs for large values of the field, *i.e.* $\phi > M_{_{\rm Pl}}$.

Hilltop models: The hilltop models are described by the potential[17]:

$$V(\phi) \simeq \Lambda^4\, \left[1 - (\phi/\mu)^p + \ldots\right]$$

and, in these models, the inflaton rolls away from an unstable equilibrium. The ellipsis indicates higher order terms that are considered to be negligible during inflation, but ensure positiveness of the potential.

[16] A. D. Linde, Phys. Lett. B **129**, 177 (1983).

[17] L. Boubekeur and D. Lyth, JCAP **0507**, 010 (2005).

[18] K. Freese, J. .A. Frieman and A. V. Olinto, Phys. Rev. Lett. **65**, 3233 (1990).

Specific inflationary models of interest I

Power law potentials: In power law potentials of the following form[16]:

$$V(\phi) = \lambda\, M_{\rm Pl}^4\, \left(\phi/M_{\rm Pl}\right)^n,$$

inflation occurs for large values of the field, *i.e.* $\phi > M_{\rm Pl}$.

Hilltop models: The hilltop models are described by the potential[17]:

$$V(\phi) \simeq \Lambda^4\, \left[1 - (\phi/\mu)^p + \ldots\right]$$

and, in these models, the inflaton rolls away from an unstable equilibrium. The ellipsis indicates higher order terms that are considered to be negligible during inflation, but ensure positiveness of the potential.

Natural inflation: In natural inflation, a non-perturbative shift symmetry is invoked to suppress radiative corrections, leading to the periodic potential[18]

$$V(\phi) = \Lambda^4\, \left[1 + \cos\left(\phi/f\right)\right],$$

where f is the scale which determines the curvature of the potential.

[16] A. D. Linde, Phys. Lett. B **129**, 177 (1983).

[17] L. Boubekeur and D. Lyth, JCAP **0507**, 010 (2005).

[18] K. Freese, J. .A. Frieman and A. V. Olinto, Phys. Rev. Lett. **65**, 3233 (1990).

Specific inflationary models of interest II

R^2 inflation: The first inflationary model proposed with the action[19]

$$S[g_{\mu\nu}] = \frac{M_{\rm Pl}^2}{2} \int {\rm d}^4x\, \sqrt{-g}\, \left(R + \frac{R^2}{6\, M^2}\right),$$

corresponds to the following potential in the Einstein frame:

$$V(\phi) = \Lambda^4\, \left(1 - {\rm e}^{-\sqrt{2/3}\,\phi/M_{\rm Pl}}\right)^2.$$

[19] A. A. Starobinsky, Phys. Lett. B **91**, 99 (1980).

[20] See, for example, R. Kallosh, A. D. Linde and D. Roest, JHEP **1311**, 198 (2013).

Specific inflationary models of interest II

R^2 inflation: The first inflationary model proposed with the action[19]

$$S[g_{\mu\nu}] = \frac{M_{\rm Pl}^2}{2} \int {\rm d}^4x\, \sqrt{-g}\, \left(R + \frac{R^2}{6\, M^2}\right),$$

corresponds to the following potential in the Einstein frame:

$$V(\phi) = \Lambda^4\, \left(1 - {\rm e}^{-\sqrt{2/3}\,\phi/M_{\rm Pl}}\right)^2.$$

α-attractors: A class of inflationary models motivated by recent developments in conformal symmetry and supergravity correspond to the potential[20]

$$V(\phi) = \Lambda^4\, \left[1 - {\rm e}^{-\sqrt{2/3}\,\phi/(\sqrt{\alpha}\, M_{\rm Pl})}\right]^2.$$

A second class of models, called the super-conformal α-attractors, are described by the following potential:

$$V(\phi) = \Lambda^4 \tanh^{2\, m}\left(\phi/\sqrt{6\, \alpha\, M_{\rm Pl}}\right).$$

[19] A. A. Starobinsky, Phys. Lett. B **91**, 99 (1980).

[20] See, for example, R. Kallosh, A. D. Linde and D. Roest, JHEP **1311**, 198 (2013).

Accounting for post-inflationary evolution

The uncertainties post-inflation are modeled by two parameters: the energy scale $\rho_{\rm th}$ by which the universe has thermalized, and the parameter $w_{\rm int}$ which characterizes the effective equation of state between the end of inflation and the energy scale specified by $\rho_{\rm th}$.

[21] A. R. Liddle and S. M. Leach, Phys. Rev. D **68**, 103503, (2003);
J. Martin and C. Ringeval, Phys. Rev. D **82**, 023511 (2010).

Accounting for post-inflationary evolution

The uncertainties post-inflation are modeled by two parameters: the energy scale $\rho_{\rm th}$ by which the universe has thermalized, and the parameter $w_{\rm int}$ which characterizes the effective equation of state between the end of inflation and the energy scale specified by $\rho_{\rm th}$.

The number of e-folds to the end of inflation is described by the expression[21]

$$N_* \approx 67 - \ln\left(\frac{k_*}{a_0\, H_0}\right) + \frac{1}{4}\,\ln\left(\frac{V_*^2}{M_{\rm Pl}^4\,\rho_{\rm end}}\right) + \frac{1-3\,w_{\rm int}}{12\,(1+w_{\rm int})}\,\ln\left(\frac{\rho_{\rm th}}{\rho_{\rm end}}\right) - \frac{1}{12}\,\ln\left(g_{\rm th}\right),$$

where $\rho_{\rm end}$ is the energy density at the end of inflation, $a_0\, H_0$ is the present Hubble scale, V_* is the potential energy when k_* left the Hubble radius during inflation, and $g_{\rm th}$ is the number of effective bosonic degrees of freedom at the energy scale $\rho_{\rm th}$.

[21] A. R. Liddle and S. M. Leach, Phys. Rev. D **68**, 103503, (2003);
J. Martin and C. Ringeval, Phys. Rev. D **82**, 023511 (2010).

Accounting for post-inflationary evolution

The uncertainties post-inflation are modeled by two parameters: the energy scale $\rho_{\rm th}$ by which the universe has thermalized, and the parameter $w_{\rm int}$ which characterizes the effective equation of state between the end of inflation and the energy scale specified by $\rho_{\rm th}$.

The number of e-folds to the end of inflation is described by the expression[21]

$$N_{*} \approx 67 - \ln\left(\frac{k_{*}}{a_0\, H_0}\right) + \frac{1}{4}\, \ln\left(\frac{V_{*}^2}{M_{\rm Pl}^4\, \rho_{\rm end}}\right) + \frac{1-3\, w_{\rm int}}{12\,(1+w_{\rm int})}\, \ln\left(\frac{\rho_{\rm th}}{\rho_{\rm end}}\right) - \frac{1}{12}\, \ln\left(g_{\rm th}\right),$$

where $\rho_{\rm end}$ is the energy density at the end of inflation, $a_0\, H_0$ is the present Hubble scale, V_{*} is the potential energy when k_{*} left the Hubble radius during inflation, and $g_{\rm th}$ is the number of effective bosonic degrees of freedom at the energy scale $\rho_{\rm th}$.

The Planck team set $k_{*} = 0.002~{\rm Mpc}^{-1}$, $g_{\rm th} = 10^3$ and a logarithmic prior was chosen on $\rho_{\rm th}$ (in the interval $[(10^3~{\rm GeV})^4, \rho_{\rm end}]$).

[21] A. R. Liddle and S. M. Leach, Phys. Rev. D **68**, 103503, (2003);
J. Martin and C. Ringeval, Phys. Rev. D **82**, 023511 (2010).

Performance of models in the n_s-r plane

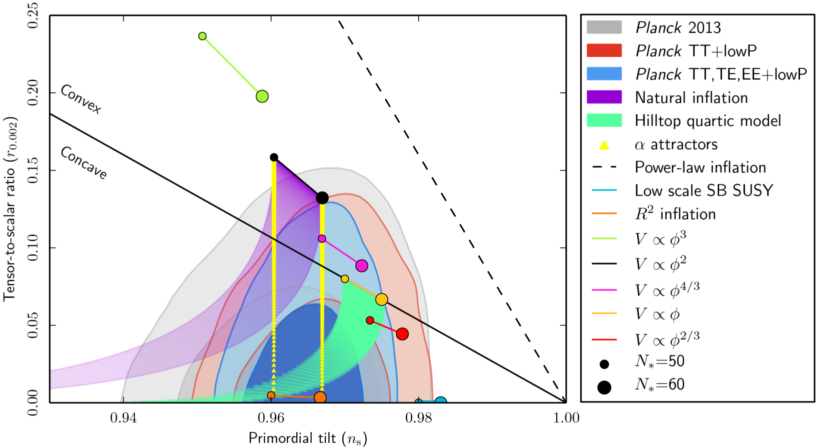

Marginalized joint $68\,\%$ and $95\,\%$ CL regions for n_s and $r_{0.002}$ from Planck in combination with other data sets, compared to the theoretical predictions of selected inflationary models[22].

[22] Planck Collaboration (P. A. R. Ade *et al.*), Astron. Astrophys. **594**, A20 (2016).

Bayesian evidence for specific inflationary models

Inflationary model	$\Delta\chi^2$		$\ln B_{0X}$	
	$w_{\rm int}=0$	$w_{\rm int}\neq 0$	$w_{\rm int}=0$	$w_{\rm int}\neq 0$
$R+R^2/(6\,M^2)$	$+0.8$	$+0.3$	$\ldots$	$+0.7$
$n=2/3$	$+6.5$	$+3.5$	-2.4	-2.3
$n=1$	$+6.2$	$+5.5$	-2.1	-1.9
$n=4/3$	$+6.4$	$+5.5$	-2.6	-2.4
$n=2$	$+8.6$	$+8.1$	-4.7	-4.6
$n=3$	$+22.8$	$+21.7$	-11.6	-11.4
$n=4$	$+43.3$	$+41.7$	-23.3	-22.7
Natural	$+7.2$	$+6.5$	-2.4	-2.3
Hilltop ($p=2$)	$+4.4$	$+3.9$	-2.6	-2.4
Hilltop ($p=4$)	$+3.7$	$+3.3$	-2.8	-2.6
Double well	$+5.5$	$+5.3$	-3.1	-2.3
Brane inflation ($p=2$)	$+3.0$	$+2.3$	-0.7	-0.9
Brane inflation ($p=4$)	$+2.8$	$+2.3$	-0.4	-0.6
Exponential inflation	$+0.8$	$+0.3$	-0.7	-0.9
SB SUSY	$+0.7$	$+0.4$	-2.2	-1.7
Supersymmetric α-model	$+0.7$	$+0.1$	-1.8	-2.0
Superconformal ($m=1$)	$+0.9$	$+0.8$	-2.3	-2.2
Superconformal ($m\neq 1$)	$+0.7$	$+0.5$	-2.4	-2.6

The improvement in the likelihood $\Delta\chi^2$ (with respect to the base ΛCDM model) and the Bayes factor (with respect to R^2 inflation) for a set of inflationary models.

Performance of inflationary models

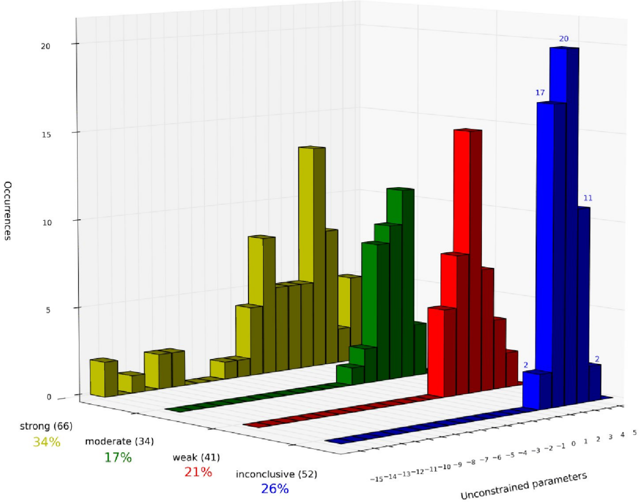

The efficiency of the inflationary paradigm leads to a situation wherein, despite the strong constraints, a variety of models continue to remain consistent with the data[23].

[23] J. Martin, C. Ringeval, R. Trotta and V. Vennin, JCAP **1403**, 039 (2014).

Power spectra with features

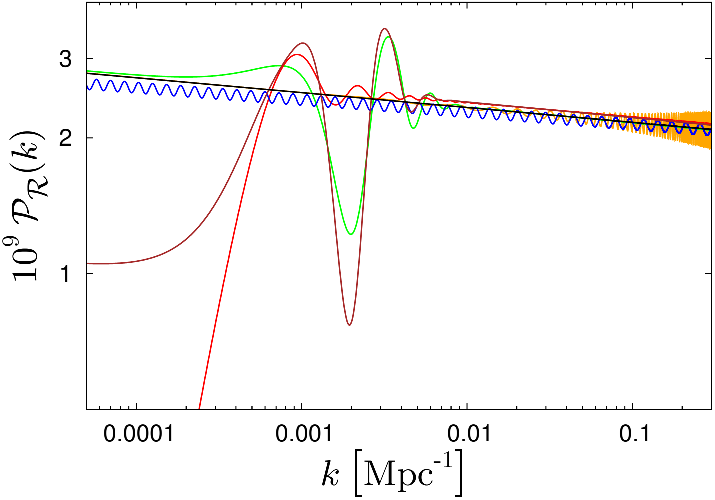

Primordial power spectra with features that lead to an improved fit to the data than the conventional, nearly scale, invariant spectra[24].

[24] Planck Collaboration (P. A. R. Ade *et al.*), Astron. Astrophys. **594**, A20 (2016).

Inflationary models permitting deviations from slow roll

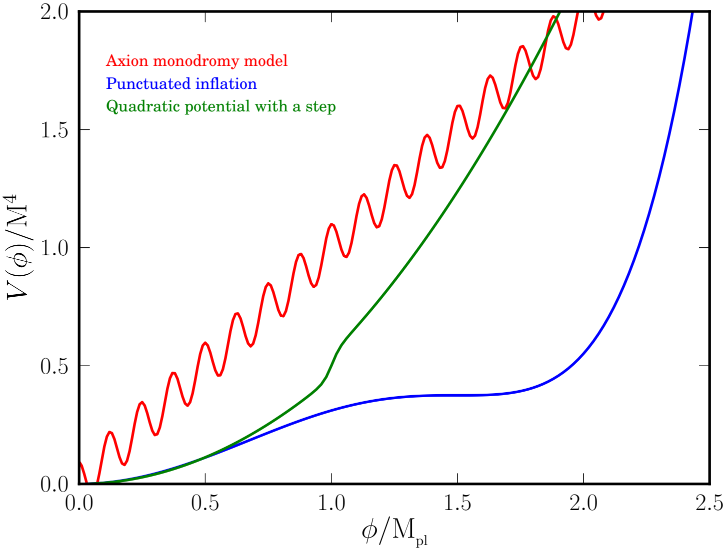

Illustration of potentials that admit departures from slow roll.

Spectra leading to an improved fit to the CMB data

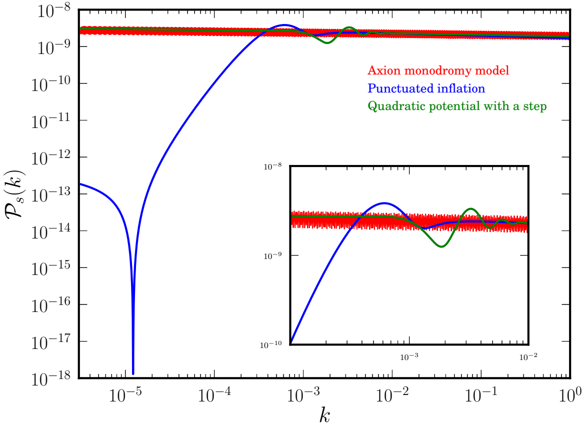

The scalar power spectra in different inflationary models that lead to a better fit to the CMB data than the conventional power law spectrum[25].

[25] R. K. Jain, P. Chingangbam, J.-O. Gong, L. Sriramkumar and T. Souradeep, JCAP **0901**, 009 (2009);
D. K. Hazra, M. Aich, R. K. Jain, L. Sriramkumar and T. Souradeep, JCAP **1010**, 008 (2010);
M. Aich, D. K. Hazra, L. Sriramkumar and T. Souradeep, Phys. Rev. D **87**, 083526 (2013).

Plan of the talk

The scalar bispectrum

The scalar bispectrum $\mathcal{B}_{\mathcal{R}\mathcal{R}\mathcal{R}}(\boldsymbol{k}_1, \boldsymbol{k}_2, \boldsymbol{k}_3)$ is related to the three point correlation function of the Fourier modes of the curvature perturbation, evaluated towards the end of inflation, say, at the conformal time $\eta_{\rm e}$, as follows[26]:

$$\langle \hat{\mathcal{R}}_{\boldsymbol{k}_1}(\eta_{\rm e})\, \hat{\mathcal{R}}_{\boldsymbol{k}_2}(\eta_{\rm e})\, \hat{\mathcal{R}}_{\boldsymbol{k}_3}(\eta_{\rm e})\rangle = (2\,\pi)^3\ \mathcal{B}_{\mathcal{R}\mathcal{R}\mathcal{R}}(\boldsymbol{k}_1, \boldsymbol{k}_2, \boldsymbol{k}_3)\ \delta^{(3)}\left(\boldsymbol{k}_1 + \boldsymbol{k}_2 + \boldsymbol{k}_3\right).$$

[26] D. Larson *et al.*, Astrophys. J. Suppl. **192**, 16 (2011);
E. Komatsu *et al.*, Astrophys. J. Suppl. **192**, 18 (2011).

The scalar bispectrum

The scalar bispectrum $\mathcal{B}_{\mathcal{R}\mathcal{R}\mathcal{R}}(\boldsymbol{k}_1, \boldsymbol{k}_2, \boldsymbol{k}_3)$ is related to the three point correlation function of the Fourier modes of the curvature perturbation, evaluated towards the end of inflation, say, at the conformal time η_{e}, as follows[26]:

$$\langle \hat{\mathcal{R}}_{\boldsymbol{k}_1}(\eta_{\mathrm{e}})\, \hat{\mathcal{R}}_{\boldsymbol{k}_2}(\eta_{\mathrm{e}})\, \hat{\mathcal{R}}_{\boldsymbol{k}_3}(\eta_{\mathrm{e}}) \rangle = (2\,\pi)^3\;\, \mathcal{B}_{\mathcal{R}\mathcal{R}\mathcal{R}}(\boldsymbol{k}_1, \boldsymbol{k}_2, \boldsymbol{k}_3)\; \delta^{(3)}\, (\boldsymbol{k}_1 + \boldsymbol{k}_2 + \boldsymbol{k}_3)\,.$$

Note that the delta function on the right hand side imposes the triangularity condition, *viz.* that the three wavevectors $\boldsymbol{k}_1$, $\boldsymbol{k}_2$ and $\boldsymbol{k}_3$ have to form the edges of a triangle.

[26] D. Larson *et al.*, Astrophys. J. Suppl. **192**, 16 (2011);
E. Komatsu *et al.*, Astrophys. J. Suppl. **192**, 18 (2011).

The scalar bispectrum

The scalar bispectrum $\mathcal{B}_{\mathcal{R}\mathcal{R}\mathcal{R}}(\boldsymbol{k}_1, \boldsymbol{k}_2, \boldsymbol{k}_3)$ is related to the three point correlation function of the Fourier modes of the curvature perturbation, evaluated towards the end of inflation, say, at the conformal time $\eta_{\rm e}$, as follows[26]:

$$\langle \hat{\mathcal{R}}_{\boldsymbol{k}_1}(\eta_{\rm e})\, \hat{\mathcal{R}}_{\boldsymbol{k}_2}(\eta_{\rm e})\, \hat{\mathcal{R}}_{\boldsymbol{k}_3}(\eta_{\rm e})\rangle = (2\,\pi)^3\; \mathcal{B}_{\mathcal{R}\mathcal{R}\mathcal{R}}(\boldsymbol{k}_1, \boldsymbol{k}_2, \boldsymbol{k}_3)\; \delta^{(3)}\,(\boldsymbol{k}_1 + \boldsymbol{k}_2 + \boldsymbol{k}_3)\,.$$

Note that the delta function on the right hand side imposes the triangularity condition, *viz.* that the three wavevectors $\boldsymbol{k}_1$, $\boldsymbol{k}_2$ and $\boldsymbol{k}_3$ have to form the edges of a triangle.

For convenience, we shall set

$$\mathcal{B}_{\mathcal{R}\mathcal{R}\mathcal{R}}(\boldsymbol{k}_1, \boldsymbol{k}_2, \boldsymbol{k}_3) = (2\,\pi)^{-9/2}\; G_{\mathcal{R}\mathcal{R}\mathcal{R}}(\boldsymbol{k}_1, \boldsymbol{k}_2, \boldsymbol{k}_3).$$

[26] D. Larson *et al.*, Astrophys. J. Suppl. **192**, 16 (2011);
E. Komatsu *et al.*, Astrophys. J. Suppl. **192**, 18 (2011).

The cubic order action governing the perturbations

It can be shown that, the third order term in the action describing the curvature perturbation is given by[27]

$$\mathcal{S}^3_{\mathcal{R}\mathcal{R}\mathcal{R}}[\mathcal{R}] = M_{\mathrm{Pl}}^2 \int \mathrm{d}\eta \int \mathrm{d}^3\boldsymbol{x} \biggl[a^2\, \epsilon_1^2\, \mathcal{R}\, \mathcal{R}'^2 + a^2\, \epsilon_1^2\, \mathcal{R}\, (\partial\mathcal{R})^2 - 2\, a\, \epsilon_1\, \mathcal{R}'\, (\partial^i\mathcal{R})\, (\partial_i\chi) + \frac{a^2}{2}\, \epsilon_1\, \epsilon_2'\, \mathcal{R}^2\, \mathcal{R}' + \frac{\epsilon_1}{2}\, (\partial^i\mathcal{R})\, (\partial_i\chi)\, (\partial^2\chi) + \frac{\epsilon_1}{4}\, (\partial^2\mathcal{R})\, (\partial\chi)^2 + \mathcal{F}_1\left(\frac{\delta\mathcal{L}^2_{\mathcal{R}\mathcal{R}}}{\delta\mathcal{R}}\right)\biggr],$$

where $\mathcal{F}_1(\delta\mathcal{L}^2_{\mathcal{R}\mathcal{R}}/\delta\mathcal{R})$ denotes terms involving the variation of the second order action with respect to $\mathcal{R}$, while χ is related to the curvature perturbation $\mathcal{R}$ through the relation

$$\partial^2\chi = a\, \epsilon_1\, \mathcal{R}'.$$

The quadratic action

[27] J. Maldacena, JHEP **0305**, 013 (2003);
D. Seery and J. E. Lidsey, JCAP **0506**, 003 (2005);
X. Chen, M.-x. Huang, S. Kachru and G. Shiu, JCAP **0701**, 002 (2007).

Evaluating the scalar bispectrum

At the leading order in the perturbations, one then finds that the scalar three-point correlation function in Fourier space is described by the integral[28]

$$\langle \hat{\mathcal{R}}_{\boldsymbol{k}_1}(\eta_{\rm e})\, \hat{\mathcal{R}}_{\boldsymbol{k}_2}(\eta_{\rm e})\, \hat{\mathcal{R}}_{\boldsymbol{k}_3}(\eta_{\rm e})\rangle = -i \int_{\eta_{\rm i}}^{\eta_{\rm e}} {\rm d}\eta\; a(\eta)\; \left\langle\left[\hat{\mathcal{R}}_{\boldsymbol{k}_1}(\eta_{\rm e})\, \hat{\mathcal{R}}_{\boldsymbol{k}_2}(\eta_{\rm e})\, \hat{\mathcal{R}}_{\boldsymbol{k}_3}(\eta_{\rm e}), \hat{H}_{\rm I}(\eta)\right]\right\rangle,$$

where $\hat{H}_{\rm I}$ is the Hamiltonian corresponding to the above third order action, while $\eta_{\rm i}$ denotes a sufficiently early time when the initial conditions are imposed on the modes, and $\eta_{\rm e}$ denotes a very late time, say, close to when inflation ends.

[28] See, for example, D. Seery and J. E. Lidsey, JCAP **0506**, 003 (2005); X. Chen, Adv. Astron. **2010**, 638979 (2010).

Evaluating the scalar bispectrum

At the leading order in the perturbations, one then finds that the scalar three-point correlation function in Fourier space is described by the integral[28]

$$\langle \hat{\mathcal{R}}_{\boldsymbol{k}_1}(\eta_{\rm e})\, \hat{\mathcal{R}}_{\boldsymbol{k}_2}(\eta_{\rm e})\, \hat{\mathcal{R}}_{\boldsymbol{k}_3}(\eta_{\rm e})\rangle = -i \int_{\eta_{\rm i}}^{\eta_{\rm e}} {\rm d}\eta\; a(\eta)\; \left\langle \left[\hat{\mathcal{R}}_{\boldsymbol{k}_1}(\eta_{\rm e})\, \hat{\mathcal{R}}_{\boldsymbol{k}_2}(\eta_{\rm e})\, \hat{\mathcal{R}}_{\boldsymbol{k}_3}(\eta_{\rm e}), \hat{H}_{\rm I}(\eta)\right]\right\rangle,$$

where $\hat{H}_{\rm I}$ is the Hamiltonian corresponding to the above third order action, while $\eta_{\rm i}$ denotes a sufficiently early time when the initial conditions are imposed on the modes, and $\eta_{\rm e}$ denotes a very late time, say, close to when inflation ends.

Note that, while the square brackets imply the commutation of the operators, the angular brackets denote the fact that the correlations are evaluated in the initial vacuum state (*viz.* the Bunch-Davies vacuum in the situation of our interest).

[28] See, for example, D. Seery and J. E. Lidsey, JCAP **0506**, 003 (2005); X. Chen, Adv. Astron. **2010**, 638979 (2010).

The non-Gaussianity parameter $f_{\rm NL}$

The observationally relevant non-Gaussianity parameter $f_{\rm NL}$ is basically introduced through the relation[29]

$$\mathcal{R}(\eta, \boldsymbol{x}) = \mathcal{R}_{\rm G}(\eta, \boldsymbol{x}) - \frac{3\, f_{\rm NL}}{5} \left[\mathcal{R}_{\rm G}^2(\eta, \boldsymbol{x}) - \langle \mathcal{R}_{\rm G}^2(\eta, \boldsymbol{x})\rangle\right],$$

where $\mathcal{R}_{\rm G}$ denotes the Gaussian quantity, and the factor of $3/5$ arises due to the relation between the Bardeen potential and the curvature perturbation during the matter dominated epoch.

[29] E. Komatsu and D. N. Spergel, Phys. Rev. D **63**, 063002 (2001).

The non-Gaussianity parameter $f_{\rm NL}$

The observationally relevant non-Gaussianity parameter $f_{\rm NL}$ is basically introduced through the relation[29]

$$\mathcal{R}(\eta, \boldsymbol{x}) = \mathcal{R}_{\rm G}(\eta, \boldsymbol{x}) - \frac{3\, f_{\rm NL}}{5}\, \left[\mathcal{R}_{\rm G}^2(\eta, \boldsymbol{x}) - \langle \mathcal{R}_{\rm G}^2(\eta, \boldsymbol{x})\rangle\right],$$

where $\mathcal{R}_{\rm G}$ denotes the Gaussian quantity, and the factor of $3/5$ arises due to the relation between the Bardeen potential and the curvature perturbation during the matter dominated epoch.

Utilizing the above relation and Wick's theorem, one can arrive at the three-point correlation function of the curvature perturbation in Fourier space in terms of the parameter $f_{\rm NL}$. It is found to be

$$\begin{aligned}\langle \hat{\mathcal{R}}_{\boldsymbol{k}_1}\, \hat{\mathcal{R}}_{\boldsymbol{k}_2}\, \hat{\mathcal{R}}_{\boldsymbol{k}_3}\rangle &= -\frac{3\, f_{\rm NL}}{10}\, (2\,\pi)^{5/2}\, \left(\frac{1}{k_1^3\, k_2^3\, k_3^3}\right)\, \delta^{(3)}(\boldsymbol{k}_1 + \boldsymbol{k}_2 + \boldsymbol{k}_3)\\ &\quad\times \left[k_1^3\, \mathcal{P}_{\rm S}(k_2)\, \mathcal{P}_{\rm S}(k_3) + \text{two permutations}\right].\end{aligned}$$

[29] E. Komatsu and D. N. Spergel, Phys. Rev. D **63**, 063002 (2001).

The relation between $f_{_{\rm NL}}$ and the scalar bispectrum

Upon making use of the above expression for the three-point function of the curvature perturbation and the definition of the scalar bispectrum, we can, in turn, arrive at the following relation[30]:

$$\begin{aligned} f_{_{\rm NL}}(\boldsymbol{k}_1,\boldsymbol{k}_2,\boldsymbol{k}_3) &= -\frac{10}{3}\,(2\,\pi)^{1/2}\,\left(k_1^3\,k_2^3\,k_3^3\right)\,\mathcal{B}_{\mathcal{R}\mathcal{R}\mathcal{R}}(\boldsymbol{k}_1,\boldsymbol{k}_2,\boldsymbol{k}_3) \\ &\quad\times\left[k_1^3\,\mathcal{P}_{_{\rm S}}(k_2)\,\mathcal{P}_{_{\rm S}}(k_3) + \text{two permutations}\right]^{-1} \\ &= -\frac{10}{3}\,\frac{1}{(2\,\pi)^4}\,\left(k_1^3\,k_2^3\,k_3^3\right)\,G_{\mathcal{R}\mathcal{R}\mathcal{R}}(\boldsymbol{k}_1,\boldsymbol{k}_2,\boldsymbol{k}_3) \\ &\quad\times\left[k_1^3\,\mathcal{P}_{_{\rm S}}(k_2)\,\mathcal{P}_{_{\rm S}}(k_3) + \text{two permutations}\right]^{-1}. \end{aligned}$$

[30] J. Martin and L. Sriramkumar, JCAP **1201**, 008 (2012).

The shape of the slow roll bispectrum

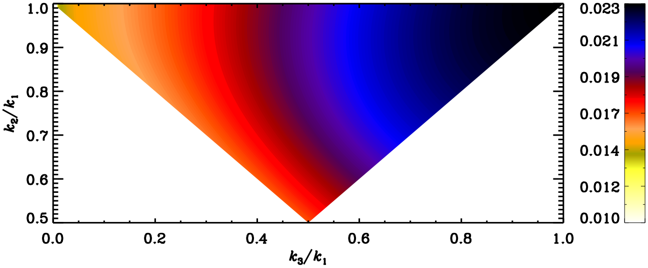

The results for the non-Gaussianity parameter $f_{\rm NL}$, evaluated analytically in the slow roll approximation, has been plotted as a function of k_3/k_1 and k_2/k_1 for the case of the popular quadratic potential. Note that the non-Gaussianity parameter peaks in the equilateral limit wherein $k_1 = k_2 = k_3$. In slow roll scenarios involving the canonical scalar field, the largest value of $f_{\rm NL}$ is found to be of the order of the first slow roll parameter ϵ_1, while $f_{\rm NL} \sim \epsilon_1/c_{\rm S}^2$ in non-canonical models, where $c_{\rm S}$ denotes the speed of the scalar perturbations[31]. The most recent results imply that $c_{\rm S} \geq 0.024$[32].

[31] See, for example, D. Seery and J. E. Lidsey, JCAP **0506**, 003 (2005); X. Chen, Adv. Astron. **2010**, 638979 (2010).

[32] P. A. R. Ade *et al.*, arXiv:1303.5084 [astro-ph.CO].

Plan of the talk

Template bispectra

For comparison with the observations, the scalar bispectrum is often expressed in terms of the parameters $f_{\rm NL}^{\rm loc}$, $f_{\rm NL}^{\rm eq}$ and $f_{\rm NL}^{\rm orth}$ as follows:

$$G_{\mathcal{RRR}}(\boldsymbol{k}_1,\boldsymbol{k}_2,\boldsymbol{k}_3) = f_{\rm NL}^{\rm loc}\, G_{\mathcal{RRR}}^{\rm loc}(\boldsymbol{k}_1,\boldsymbol{k}_2,\boldsymbol{k}_3) + f_{\rm NL}^{\rm eq}\, G_{\mathcal{RRR}}^{\rm eq}(\boldsymbol{k}_1,\boldsymbol{k}_2,\boldsymbol{k}_3) + f_{\rm NL}^{\rm orth}\, G_{\mathcal{RRR}}^{\rm orth}(\boldsymbol{k}_1,\boldsymbol{k}_2,\boldsymbol{k}_3).$$

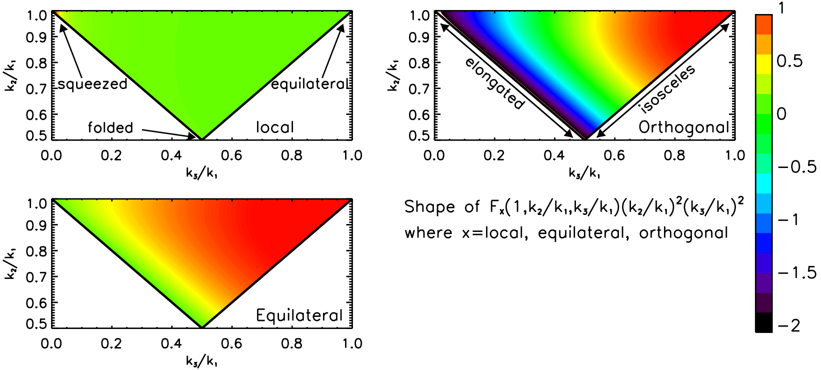

Illustration of the three template basis bispectra[33].

[33] E. Komatsu, Class. Quantum Grav. **27**, 124010 (2010).

Constraints on the scalar non-Gaussianity parameters

The constraints on the primordial values of the non-Gaussianity parameters from the Planck data are as follows[34]:

$$
\begin{aligned}
f_{\rm NL}^{\rm loc} &= 0.8 \pm 5.0,\\
f_{\rm NL}^{\rm eq} &= -4 \pm 43,\\
f_{\rm NL}^{\rm orth} &= -26 \pm 21.
\end{aligned}
$$

[34] Planck Collaboration (P. A. R. Ade *et al.*), Astron. Astrophys. **594**, A17 (2016).

Constraints on the scalar non-Gaussianity parameters

The constraints on the primordial values of the non-Gaussianity parameters from the Planck data are as follows[34]:

$$\begin{aligned} f_{\rm NL}^{\rm loc} &= 0.8 \pm 5.0, \\ f_{\rm NL}^{\rm eq} &= -4 \pm 43, \\ f_{\rm NL}^{\rm orth} &= -26 \pm 21. \end{aligned}$$

It should be stressed that these are constraints on the primordial values.

[34] Planck Collaboration (P. A. R. Ade *et al.*), Astron. Astrophys. **594**, A17 (2016).

Constraints on the scalar non-Gaussianity parameters

The constraints on the primordial values of the non-Gaussianity parameters from the Planck data are as follows[34]:

$$
\begin{aligned}
f_{\rm NL}^{\rm loc} &= 0.8 \pm 5.0, \\
f_{\rm NL}^{\rm eq} &= -4 \pm 43, \\
f_{\rm NL}^{\rm orth} &= -26 \pm 21.
\end{aligned}
$$

It should be stressed that these are constraints on the primordial values.

Also, the constraints on each of the $f_{\rm NL}$ parameters have been arrived at assuming that the other two parameters are zero.

[34] Planck Collaboration (P. A. R. Ade *et al.*), Astron. Astrophys. **594**, A17 (2016).

Constraints on the scalar non-Gaussianity parameters

The constraints on the primordial values of the non-Gaussianity parameters from the Planck data are as follows[34]:

$$\begin{aligned} f_{\rm NL}^{\rm loc} &= 0.8 \pm 5.0, \\ f_{\rm NL}^{\rm eq} &= -4 \pm 43, \\ f_{\rm NL}^{\rm orth} &= -26 \pm 21. \end{aligned}$$

It should be stressed that these are constraints on the primordial values.

Also, the constraints on each of the $f_{\rm NL}$ parameters have been arrived at assuming that the other two parameters are zero.

These constraints imply that slowly rolling single field models involving the canonical scalar field which are favored by the data at the level of power spectra are also consistent with the data at the level of non-Gaussianities.

[34] Planck Collaboration (P. A. R. Ade *et al.*), Astron. Astrophys. **594**, A17 (2016).

Constraints on the scalar non-Gaussianity parameters

The constraints on the primordial values of the non-Gaussianity parameters from the Planck data are as follows[34]:

$$
\begin{aligned}
f_{\rm NL}^{\rm loc} &= 0.8 \pm 5.0,\\
f_{\rm NL}^{\rm eq} &= -4 \pm 43,\\
f_{\rm NL}^{\rm orth} &= -26 \pm 21.
\end{aligned}
$$

It should be stressed that these are constraints on the primordial values.

Also, the constraints on each of the $f_{\rm NL}$ parameters have been arrived at assuming that the other two parameters are zero.

These constraints imply that slowly rolling single field models involving the canonical scalar field which are favored by the data at the level of power spectra are also consistent with the data at the level of non-Gaussianities.

We should also add that these constraints become less stringent if the primordial spectra are assumed to contain features.

[34] Planck Collaboration (P. A. R. Ade *et al.*), Astron. Astrophys. **594**, A17 (2016).

Plan of the talk

The various times of interest[35]

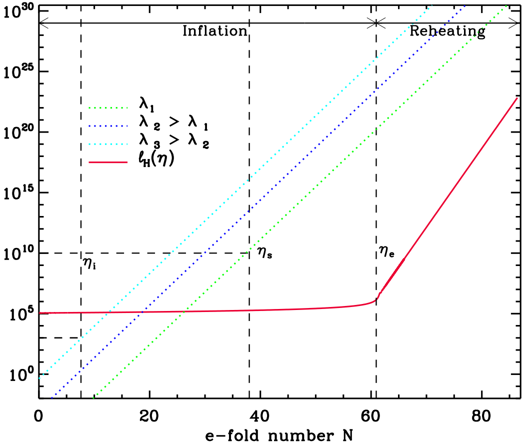

The exact behavior of the physical wavelengths and the Hubble radius plotted as a function of the number of e-folds in the case of the archetypical quadratic potential, which allows us to illustrate the various times of our interest, *viz.* $\eta_{\rm i}$, $\eta_{\rm s}$ and $\eta_{\rm e}$.

[35] D. K. Hazra, L. Sriramkumar and J. Martin, JCAP **1305**, 026 (2013).

Results from BINGO

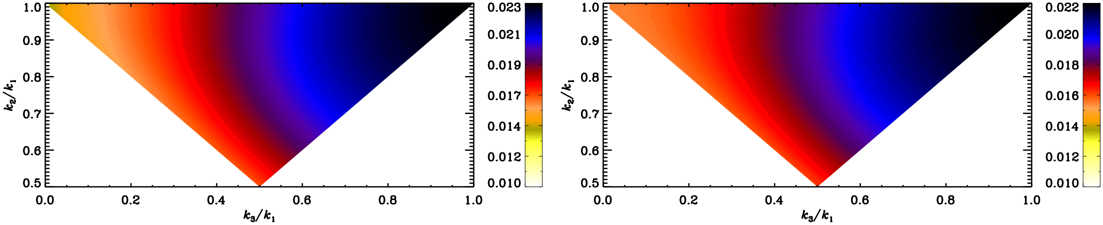

A comparison of the analytical results (on the left) for the non-Gaussianity parameter $f_{\rm NL}$ with the numerical results from the code BIspectra and Non-Gaussianity Operator or, simply, BINGO (on the right) for a generic triangular configuration of the wavevectors in the case of the standard quadratic potential[36] The maximum difference between the numerical and the analytic results is found to be about 5%.

[36] D. K. Hazra, L. Sriramkumar and J. Martin, JCAP **1305**, 026, (2013).

$f_{\rm NL}$ in models with features

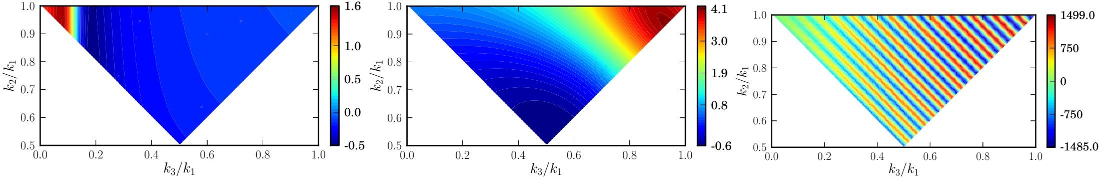

The scalar non-Gaussianity parameter $f_{\rm NL}$ in the punctuated inflationary scenario (on the left), quadratic potential with a step (in the middle) and the axion monodromy model (on the right)[37].

[37] D. K. Hazra, L. Sriramkumar and J. Martin, JCAP **1305**, 026 (2013);
V. Sreenath, D. K. Hazra and L. Sriramkumar, JCAP **1502**, 029 (2015).

The inflationary scalar bispectrum

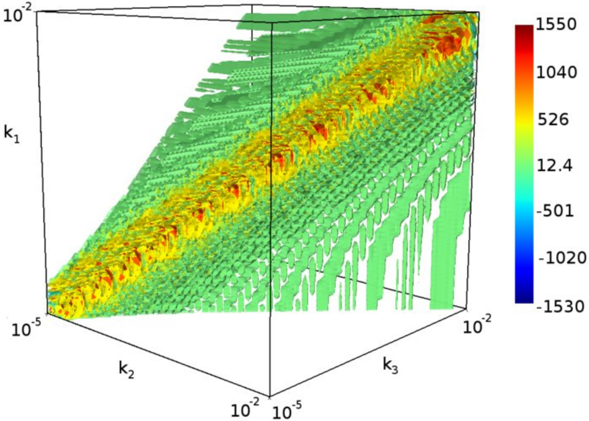

The shape of the inflationary scalar bispectrum (actually, the non-Gaussianity parameter $f_{\rm NL}$) in the case of the axion monodromy model[38].

[38] V. Sreenath, D. K. Hazra and L. Sriramkumar, JCAP **1502**, 029 (2015).

Plan of the talk

Bouncing scenarios as an alternative paradigm[39]

- Bouncing models correspond to situations wherein the universe initially goes through a period of contraction until the scale factor reaches a certain minimum value before transiting to the expanding phase.

[39] See, for instance, M. Novello and S. P. Bergliaffa, Phys. Rep. **463**, 127 (2008); D. Battefeld and P. Peter, Phys. Rep. **571**, 1 (2015).

Bouncing scenarios as an alternative paradigm[39]

- Bouncing models correspond to situations wherein the universe initially goes through a period of contraction until the scale factor reaches a certain minimum value before transiting to the expanding phase.
- They offer an alternative to inflation to overcome the horizon problem, as they permit well motivated, Minkowski-like initial conditions to be imposed on the perturbations at early times during the contracting phase.

[39] See, for instance, M. Novello and S. P. Bergliaffa, Phys. Rep. **463**, 127 (2008); D. Battefeld and P. Peter, Phys. Rep. **571**, 1 (2015).

Bouncing scenarios as an alternative paradigm[39]

- Bouncing models correspond to situations wherein the universe initially goes through a period of contraction until the scale factor reaches a certain minimum value before transiting to the expanding phase.
- They offer an alternative to inflation to overcome the horizon problem, as they permit well motivated, Minkowski-like initial conditions to be imposed on the perturbations at early times during the contracting phase.
- However, matter fields *will* have to violate the null energy condition near the bounce in order to give rise to such a scale factor. Also, there exist (genuine) concerns whether such an assumption about the scale factor is valid in a domain where general relativity can be supposed to fail and quantum gravitational effects are expected to take over.

[39] See, for instance, M. Novello and S. P. Bergliaffa, Phys. Rep. **463**, 127 (2008); D. Battefeld and P. Peter, Phys. Rep. **571**, 1 (2015).

Overcoming the horizon problem in bouncing models

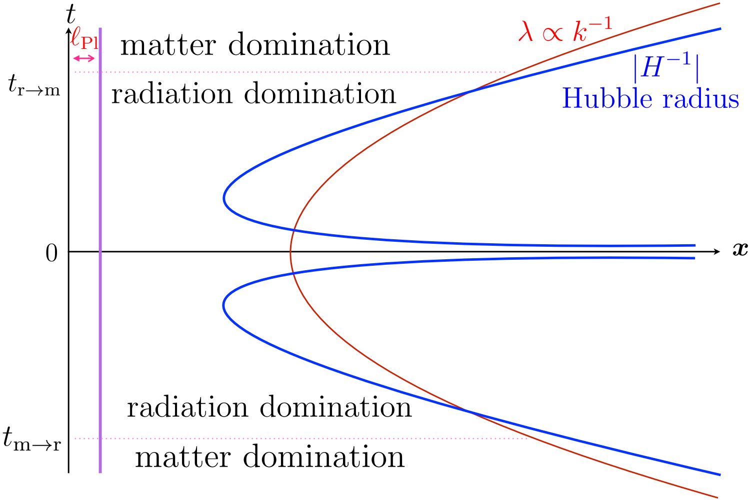

Behavior in inflation

Evolution of the physical wavelength and the Hubble radius in a bouncing scenario[40].

[40] Figure from, D. Battefeld and P. Peter, Phys. Rept. **571**, 1 (2015).

Violation of the null energy condition near the bounce

Recall that, according to the Friedmann equations

$$\dot{H} = -4\,\pi\,G\,(\rho + p)\,.$$

In any bouncing scenario, the Hubble parameter is negative before the bounce, crosses zero at the bounce and is positive thereafter.

Violation of the null energy condition near the bounce

Recall that, according to the Friedmann equations

$$\dot{H} = -4\,\pi\,G\,(\rho + p)\,.$$

In any bouncing scenario, the Hubble parameter is negative before the bounce, crosses zero at the bounce and is positive thereafter.

It can be shown that, if the modes of cosmological interest have to be inside the Hubble radius at early times during the contracting phase, *the universe needs to undergo non-accelerated contraction*.

Violation of the null energy condition near the bounce

Recall that, according to the Friedmann equations

$$\dot{H} = -4\,\pi\,G\,(\rho + p)\,.$$

In any bouncing scenario, the Hubble parameter is negative before the bounce, crosses zero at the bounce and is positive thereafter.

It can be shown that, if the modes of cosmological interest have to be inside the Hubble radius at early times during the contracting phase, *the universe needs to undergo non-accelerated contraction*.

In such cases, one finds that $\dot{H}$ *will* be positive near the bounce, which implies that $\rho + p < 0$ in this domain. In other words, the null energy condition needs to be violated in order to achieve such bounces.

Behavior during inflation

A new model for the completely symmetric matter bounce

The so-called matter bounce scenario is described by the scale factor

$$a(\eta) = a_0\, \left(1 + \eta^2/\eta_0^2\right) = a_0\, \left(1 + k_0^2\, \eta^2\right).$$

It can be driven with the aid of two fluids, one which is matter and another fluid which behaves like radiation, but has negative energy density.

[41] R. N. Raveendran, D. Chowdhury and L. Sriramkumar, arXiv:1703.10061v1 [gr-qc].

A new model for the completely symmetric matter bounce

The so-called matter bounce scenario is described by the scale factor

$$a(\eta) = a_0\,\left(1+\eta^2/\eta_0^2\right) = a_0\,\left(1+k_0^2\,\eta^2\right).$$

It can be driven with the aid of two fluids, one which is matter and another fluid which behaves like radiation, but has negative energy density.

We find that the behavior can also be achieved with the help of two scalar fields, say, ϕ and χ, that are governed by the following action[41]:

$$S[\phi,\chi] = -\int \mathrm{d}^4x\,\sqrt{-g}\,\left[\frac{1}{2}\,\partial_\mu\phi\,\partial^\mu\phi + V(\phi) + U_0\,\left(-\frac{1}{2}\,\partial_\mu\chi\,\partial^\mu\chi\right)^2\right],$$

where U_0 is a constant and the potential $V(\phi)$ is given by

$$V(\phi) = \frac{6\,M_{_{\mathrm{Pl}}}^2\,(k_0^2/a_0^2)}{\cosh^6[\phi/(\sqrt{12}\,M_{_{\mathrm{Pl}}})]}.$$

[41] R. N. Raveendran, D. Chowdhury and L. Sriramkumar, arXiv:1703.10061v1 [gr-qc].

Evolution of $\mathcal{R}_k$, $\mathcal{S}_k$ and h_k

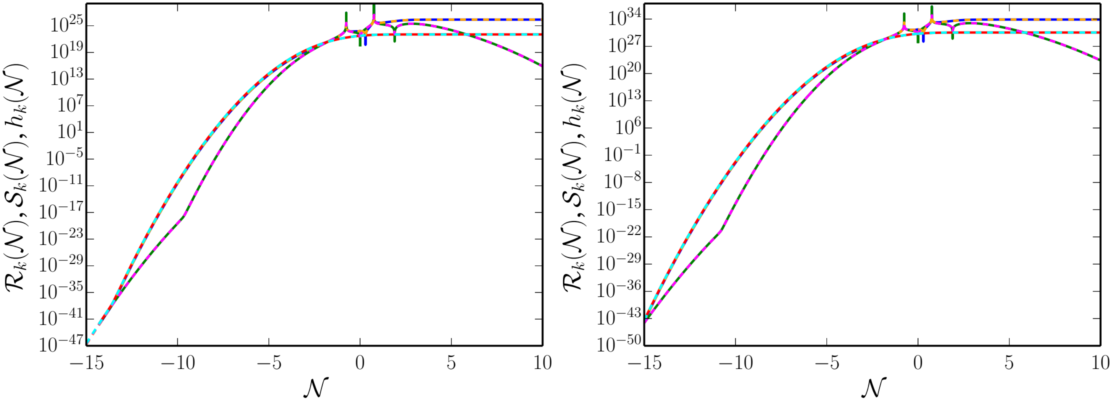

The evolution of the curvature, isocurvature and tensor perturbations, *viz.* $\mathcal{R}_k$ (in blue and orange), $\mathcal{S}_k$ (in green and magenta) and h_k (in red and cyan) across the bounce for the modes $k/k_0 = 10^{-20}$ (on the left) and $k/k_0 = 10^{-25}$ (on the right). We have set $k_0 = M_{\rm Pl}$, $a_0 = 3 \times 10^7$, $\alpha = 10^5$ and $\beta = 10^2$. The solid lines denote the results obtained numerically, while the dashed lines represent the analytical approximations.

The scalar and tensor power spectra in the matter bounce

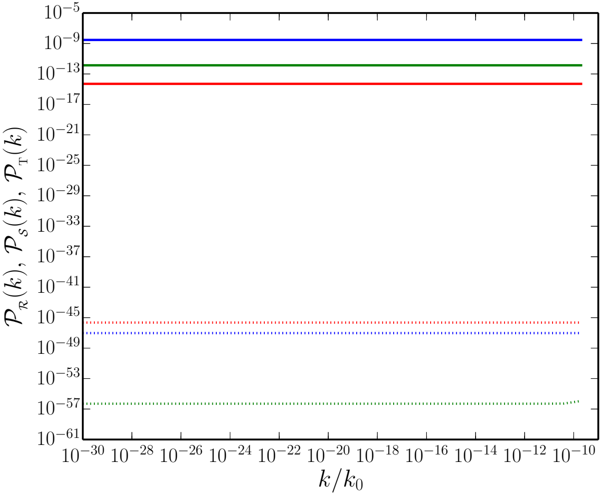

The scalar (curvature as blue and isocurvature as green) and tensor (as red) power spectra have been plotted before (as dotted lines) as well as after (as solid lines) the bounce[42].

[42] R. N. Raveendran, D. Chowdhury and L. Sriramkumar, arXiv:1703.10061v1 [gr-qc].

The evolution of the tensor-to-scalar ratio

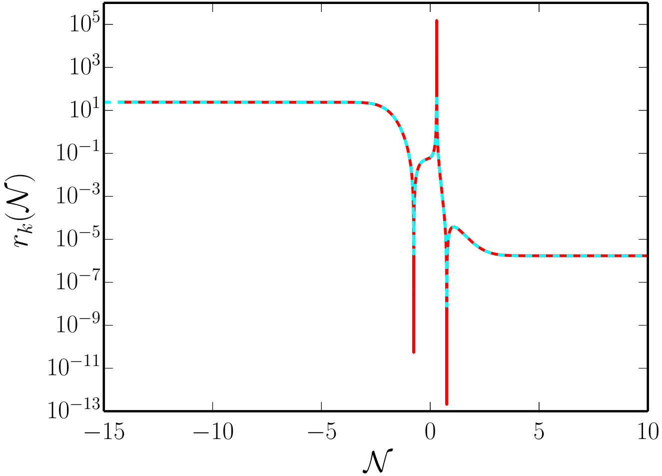

The evolution of the tensor-to-scalar ratio r across the symmetric matter bounce for a typical mode of cosmological interest. The solid (in red) and dashed (in cyan) lines represent the numerical and analytical results, respectively.

Plan of the talk

Summary: The inflationary scenario

- A nearly scale invariant primordial spectrum as is generated in slow roll inflation is remarkably consistent with the cosmological data.

[43] J. Martin, C. Ringeval and V. Vennin, Phys. Dark Univ. **5–6**, 75 (2014).

[44] J. R. Fergusson, H. F. Gruetjen, E. P. S. Shellard and M. Liguori, Phys. Rev. D **91**, 023502 (2015).

Summary: The inflationary scenario

- A nearly scale invariant primordial spectrum as is generated in slow roll inflation is remarkably consistent with the cosmological data.
- The strong constraints on the scalar non-Gaussianity parameter seem to further support slow roll models of inflation.

[43] J. Martin, C. Ringeval and V. Vennin, Phys. Dark Univ. **5–6**, 75 (2014).

[44] J. R. Fergusson, H. F. Gruetjen, E. P. S. Shellard and M. Liguori, Phys. Rev. D **91**, 023502 (2015).

Summary: The inflationary scenario

- A nearly scale invariant primordial spectrum as is generated in slow roll inflation is remarkably consistent with the cosmological data.
- The strong constraints on the scalar non-Gaussianity parameter seem to further support slow roll models of inflation.
- While there exist some anomalies (features in the power spectra, hemispherical asymmetry, etc.), they do not seem to have substantial statistical significance.

[43] J. Martin, C. Ringeval and V. Vennin, Phys. Dark Univ. **5–6**, 75 (2014).

[44] J. R. Fergusson, H. F. Gruetjen, E. P. S. Shellard and M. Liguori, Phys. Rev. D **91**, 023502 (2015).

Summary: The inflationary scenario

- A nearly scale invariant primordial spectrum as is generated in slow roll inflation is remarkably consistent with the cosmological data.
- The strong constraints on the scalar non-Gaussianity parameter seem to further support slow roll models of inflation.
- While there exist some anomalies (features in the power spectra, hemispherical asymmetry, etc.), they do not seem to have substantial statistical significance.
- One may need to carry out a systematic search involving the scalar and the tensor power spectra[43], the scalar and the tensor bispectra and the cross correlations to arrive at a smaller subset of viable inflationary models[44].

[43] J. Martin, C. Ringeval and V. Vennin, Phys. Dark Univ. **5–6**, 75 (2014).

[44] J. R. Fergusson, H. F. Gruetjen, E. P. S. Shellard and M. Liguori, Phys. Rev. D **91**, 023502 (2015).

Can inflation be falsified?

The difficulty with the inflationary paradigm

A theory that predicts everything predicts nothing[a].

[a] P. J. Steinhardt, Sci. Am. **304**, 36 (2011).

Bayesian evidence for models across paradigms

As the recent hiccups in CMB polarization observations demonstrated, whatever the data turns out to be it will be paraded as proof of inflation. This is because for any observation there is an inflationary model fitting it. Concomitantly, there is a trend in parroting the death of inflation's alternatives (such as cyclic models, string gas cosmology and varying speed of light models).

Putting aside sociology, these perceptions may derive from an important scientific issue. We argued here that the oft-used concept of Bayesian evidence fails to adequately capture the tenet that falsifiability is the hallmark of a scientific theory. Whilst the concept may be perfectly appropriate for comparing models within a paradigm, it fails to suitably penalize the whole paradigm for not making a prediction that could rule it out[a].

[a] G. Gubitosi, M. Lagos, J. Magueijo and R. Allison, JCAP **06**, 002 (2016).

Summary: The bouncing models

- Earlier efforts had seemed to suggest that the tensor-to-scalar ratio may naturally be large in symmetric bounces.

Summary: The bouncing models

- Earlier efforts had seemed to suggest that the tensor-to-scalar ratio may naturally be large in symmetric bounces.
- We have been able to construct a *completely* symmetric matter bounce scenario that leads to scale invariant spectra and a tensor-to-scalar ratio that is consistent with the observations.

Summary: The bouncing models

- Earlier efforts had seemed to suggest that the tensor-to-scalar ratio may naturally be large in symmetric bounces.
- We have been able to construct a *completely* symmetric matter bounce scenario that leads to scale invariant spectra and a tensor-to-scalar ratio that is consistent with the observations.
- We are currently working on constructing symmetric bouncing models that lead to scalar power spectra with a tilt as suggested by the cosmological data.

Summary: The bouncing models

- Earlier efforts had seemed to suggest that the tensor-to-scalar ratio may naturally be large in symmetric bounces.
- We have been able to construct a *completely* symmetric matter bounce scenario that leads to scale invariant spectra and a tensor-to-scalar ratio that is consistent with the observations.
- We are currently working on constructing symmetric bouncing models that lead to scalar power spectra with a tilt as suggested by the cosmological data.
- It is also important to examine if the non-Gaussianities generated in such models are in agreement with the recent constraints from Planck.

Issues confronting bouncing models

- In inflation, any classical perturbations present at the start will decay. In contrast, they grow strongly in bouncing models. So, these need to be assumed to be rather small if smooth bounces have to begin.

[45] L. E. Allen and D. Wands, Phys. Rev. **70**, 063515 (2004).

[46] Y-F. Cai, R. Brandenberger and X. Zhang, Phys. Letts. B **703**, 25 (2011).

[47] J. Quintin, Z. Sherkatghanad, Y-F. Cai and R. Brandenberger, Phys. Rev. D **92**, 062532 (2015).

Issues confronting bouncing models

- In inflation, any classical perturbations present at the start will decay. In contrast, they grow strongly in bouncing models. So, these need to be assumed to be rather small if smooth bounces have to begin.
- The growth of the perturbations as one approaches the bounce during the contracting phase causes concerns about the validity of linear perturbation theory near the bounce. Is it, for instance, sufficient if the perturbations remain small in specific gauges? Is a divergent curvature perturbation acceptable?

[45] L. E. Allen and D. Wands, Phys. Rev. **70**, 063515 (2004).

[46] Y-F. Cai, R. Brandenberger and X. Zhang, Phys. Letts. B **703**, 25 (2011).

[47] J. Quintin, Z. Sherkatghanad, Y-F. Cai and R. Brandenberger, Phys. Rev. D **92**, 062532 (2015).

Issues confronting bouncing models

- In inflation, any classical perturbations present at the start will decay. In contrast, they grow strongly in bouncing models. So, these need to be assumed to be rather small if smooth bounces have to begin.
- The growth of the perturbations as one approaches the bounce during the contracting phase causes concerns about the validity of linear perturbation theory near the bounce. Is it, for instance, sufficient if the perturbations remain small in specific gauges? Is a divergent curvature perturbation acceptable?
- Is it possible to construct wider classes of completely symmetric bounces with nearly scale invariant spectra and viable tensor-to-scalar ratios[45]?

[45] L. E. Allen and D. Wands, Phys. Rev. **70**, 063515 (2004).

[46] Y-F. Cai, R. Brandenberger and X. Zhang, Phys. Letts. B **703**, 25 (2011).

[47] J. Quintin, Z. Sherkatghanad, Y-F. Cai and R. Brandenberger, Phys. Rev. D **92**, 062532 (2015).

Issues confronting bouncing models

- In inflation, any classical perturbations present at the start will decay. In contrast, they grow strongly in bouncing models. So, these need to be assumed to be rather small if smooth bounces have to begin.
- The growth of the perturbations as one approaches the bounce during the contracting phase causes concerns about the validity of linear perturbation theory near the bounce. Is it, for instance, sufficient if the perturbations remain small in specific gauges? Is a divergent curvature perturbation acceptable?
- Is it possible to construct wider classes of completely symmetric bounces with nearly scale invariant spectra and viable tensor-to-scalar ratios[45]?
- After the bounce, the universe needs to transit to a radiation dominated epoch. How can this be achieved? Does this process affect the evolution of the large scale perturbations[46]?

[45] L. E. Allen and D. Wands, Phys. Rev. **70**, 063515 (2004).

[46] Y-F. Cai, R. Brandenberger and X. Zhang, Phys. Letts. B **703**, 25 (2011).

[47] J. Quintin, Z. Sherkatghanad, Y-F. Cai and R. Brandenberger, Phys. Rev. D **92**, 062532 (2015).

Issues confronting bouncing models

- In inflation, any classical perturbations present at the start will decay. In contrast, they grow strongly in bouncing models. So, these need to be assumed to be rather small if smooth bounces have to begin.
- The growth of the perturbations as one approaches the bounce during the contracting phase causes concerns about the validity of linear perturbation theory near the bounce. Is it, for instance, sufficient if the perturbations remain small in specific gauges? Is a divergent curvature perturbation acceptable?
- Is it possible to construct wider classes of completely symmetric bounces with nearly scale invariant spectra and viable tensor-to-scalar ratios[45]?
- After the bounce, the universe needs to transit to a radiation dominated epoch. How can this be achieved? Does this process affect the evolution of the large scale perturbations[46]?
- Does the growth in the amplitude of the perturbations as one approaches the bounce naturally lead to large levels of non-Gaussianities in such models[47]?

[45] L. E. Allen and D. Wands, Phys. Rev. **70**, 063515 (2004).

[46] Y-F. Cai, R. Brandenberger and X. Zhang, Phys. Letts. B **703**, 25 (2011).

[47] J. Quintin, Z. Sherkatghanad, Y-F. Cai and R. Brandenberger, Phys. Rev. D **92**, 062532 (2015).

Collaborators I

Rajeev Kumar Jain

Dhiraj Kumar Hazra

Moumita Aich

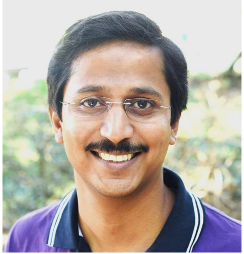

V. Sreenath

Debika Chowdhury

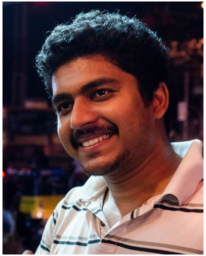

Rathul Nath Raveendran

Collaborators II

Pravabati Chingangbam

Jinn-Ouk Gong

Rakesh Tibrewala

Tarun Souradeep

Jérôme Martin

Thank you for your attention